

SELF AND NONSELF RECOGNITION WITH BACTERIAL AND ANIMAL GLYCANS, SURVEYS BY SYNTHETIC CHEMISTRY

Yukari Fujimoto, Katsunori Tanaka, Atsushi Shimoyama, and Koichi Fukase

Contents

1. Overview	324
2. Bacterial Glycoconjugates for Nonself Recognition—Lipopolysaccharide (LPS)	325
3. Synthesis of <i>H. pylori</i> Kdo–Lipid A Backbone	327
4. Glycosylation with Kdo Donor 11	327
5. Cytokine (IL-6) Induction in Human Peripheral Whole-Blood Cell Cultures	328
6. Bacterial Glycoconjugates for Nonself Recognition—Peptidoglycan (PGN)	329
7. Synthesis of Disaccharide Moiety 15 in Tracheal Cytotoxin with β -Selective Glycosylation	331
8. Synthesis of Tracheal Cytotoxin 20 and Its Fragment 21	332
9. Immunostimulatory Activities of DAP Containing PGN Fragments	333
10. Visualizing the <i>In Vivo</i> Dynamics of Animal <i>N</i> -Glycans	333
11. PET Imaging of Glycoproteins	334
12. Method for ^{68}Ga -DOTA Labeling and MicroPET Imaging in Rabbit	335
13. PET Imaging of Glycoclusters	337
14. Method for Preparation of <i>N</i> -Glycan Clusters and PET Imaging in Mouse	338
Acknowledgments	339
References	340

Abstract

In this chapter, we describe synthetic studies on partial structures of lipopolysaccharide (LPS) and peptidoglycan (PGN), which work as tags for nonself recognition in innate immune system. Our previous studies demonstrated that

Department of Chemistry, Graduate School of Science, Osaka University, Machikaneyama, Toyonaka, Osaka, Japan

lipid A is the endotoxic principle of LPS. The synthetic homogeneous preparations have enabled not only precise structure–activity relationships, but also recognition mechanisms of LPS with innate immune receptor complexes, including the TLR4/MD-2 complex, to be studied. Synthetic studies of lipid A and Kdo–lipid A from parasitic *Helicobacter pylori* revealed their low inflammatory activities, suggesting the molecular evolution to escape from the host immune system. A synthetic study of the partial structures of PGN has also contributed to the understanding of the innate immune mechanism. The biological activities of the synthetic fragments have revealed that the intracellular receptor Nod2 recognizes partial structures containing the muramyl dipeptide (MDP) moiety. The PGN of Gram-negative bacteria and some Gram-positive bacteria contain *meso*-diaminopimelic acid (*meso*-DAP), and recent studies have revealed that the intracellular receptor Nod1 recognizes DAP-containing peptides. We have synthesized DAP-containing PGN fragments, including the first chemical synthesis of tracheal cytotoxin (TCT). The ability of these fragments to stimulate human Nod1 as well as differences in Nod1 recognition for various synthesized ligand structures was elucidated. Cell-surface glycans such as *N*-glycans and *O*-glycans on glycoproteins and glycoconjugates work as signaling molecules for self-recognition and control immune system. Our new strategy using glycan-imaging in whole-body system is expected to unveil the dynamics of glycans in the body. Positron emission tomography (PET) is a noninvasive method that visualizes the locations and levels of radiotracer accumulation. We developed the facile labeling of peptides and proteins for PET imaging. The labeled glycoproteins and glycoclusters were then subjected to PET imaging in order to examine their *in vivo* dynamics, visualizing the differences in the circulatory residence of glycoproteins and glycoclusters in the presence or absence of sialic acid residues.

1. OVERVIEW

Self and nonself recognition is a fundamental function to maintain the life of a multicellular organism with preventing the invasion of microorganisms, components from other species/individuals, or problematic materials. In order to distinguish the difference between self and nonself, glycan structures or glycoconjugates on the cell surface are often used as the signal motifs. One of significant roles in nonself recognition is to recognize microorganism including bacteria, which has recently been exhibited to have close relationships with the innate immunity activation. On the other hand, the cell/cell and cell/protein interactions mediated by the *N*-glycans, for example, stimulating the immunosuppressive signals through Siglec families, constitute the significant roles in self-recognition process. In this chapter, we show key chemical synthesis methods to build a compound library of bacterial glycoconjugates, and the immunostimulating functions.

In addition, the methods for visualizing the *in vivo* dynamics of *N*-glycans and glycoproteins, by means of the noninvasive molecular imaging as the new tool for investigating the oligosaccharides functions, will be described.

2. BACTERIAL GLYCOCONJUGATES FOR NONSELF RECOGNITION — LIPOPOLYSACCHARIDE (LPS)

LPS of Gram-negative bacteria is one of major signaling motifs for the recognition of bacteria invading to the host organism. The compound is also known as endotoxin due to its potent immunostimulation and the toxicity. LPS is recognized with Toll-like receptor 4 (TLR4)/MD-2 complex on cell surface to produce mediators, for example, cytokines, prostaglandins, the platelet activating factor, oxygen-free radicals, and NO, which all activate and modulate the immune system (Kusumoto and Fukase, 2006; Raetz and Whitfield, 2002). LPS consists of a glycolipid component named lipid A, which is covalently connected to the polysaccharide part. Lipid As from various bacteria have common structural features, that is, GlcNAc β (1-6)GlcNAc possessing phosphono groups at the reducing end and 4-position of the nonreducing glucosamine, and long-chain acyl groups at 2, 2', 3, and 3' positions. The total synthesis of *Escherichia coli* lipid A **1** (synthetic **1** is termed 506) confirmed that lipid A is the chemical entity responsible for the innate immunostimulatory activity of LPS (Fig. 16.1) (Kusumoto and Fukase, 2006). Various lipid A structures are known such as compound **2**, **3**, **4**, and **5** (Fig. 16.1) (Kusumoto *et al.*, 1999, 2009; Takada and Kotani, 1992), and we have synthesized various natural or designed lipid A structures to investigate the structure-activity relationships and analyze the action mechanisms (Fujimoto *et al.*, 2005).

One of the characteristic groups of lipid As are the compounds from parasitic bacteria such as *Helicobacter pylori* and *Porphyromonas gingivalis*. *H. pylori* is one of Gram-negative bacteria and an etiological agent of gastroduodenal diseases, including chronic gastritis, gastroduodenal ulcers, and gastric cancer. *H. pylori* LPS shows a lower endotoxic activity compared to other enterobacterial preparations such as *E. coli* LPS, but it is considered to have relationships to the chronic inflammation. *H. pylori* LPS has characteristic lipid A structures; namely it has fewer but longer acyl groups, and does not have the 4'-phosphate group, and the glycosyl phosphate often has an ethanolamine group (**8b**; Fig. 16.1). *H. pylori* LPS has one Kdo as a linkage between lipid A and the polysaccharide part. We have synthesized triacyl type *H. pylori* lipid A with or without ethanolamine (**8a**, **8b**) (Fujimoto *et al.*, 2007; Sakai *et al.*, 2000), and also *H. pylori* lipid A connecting to one Kdo residue (**9**) (Fujimoto *et al.*, 2007), in order to elucidate their biological activities.

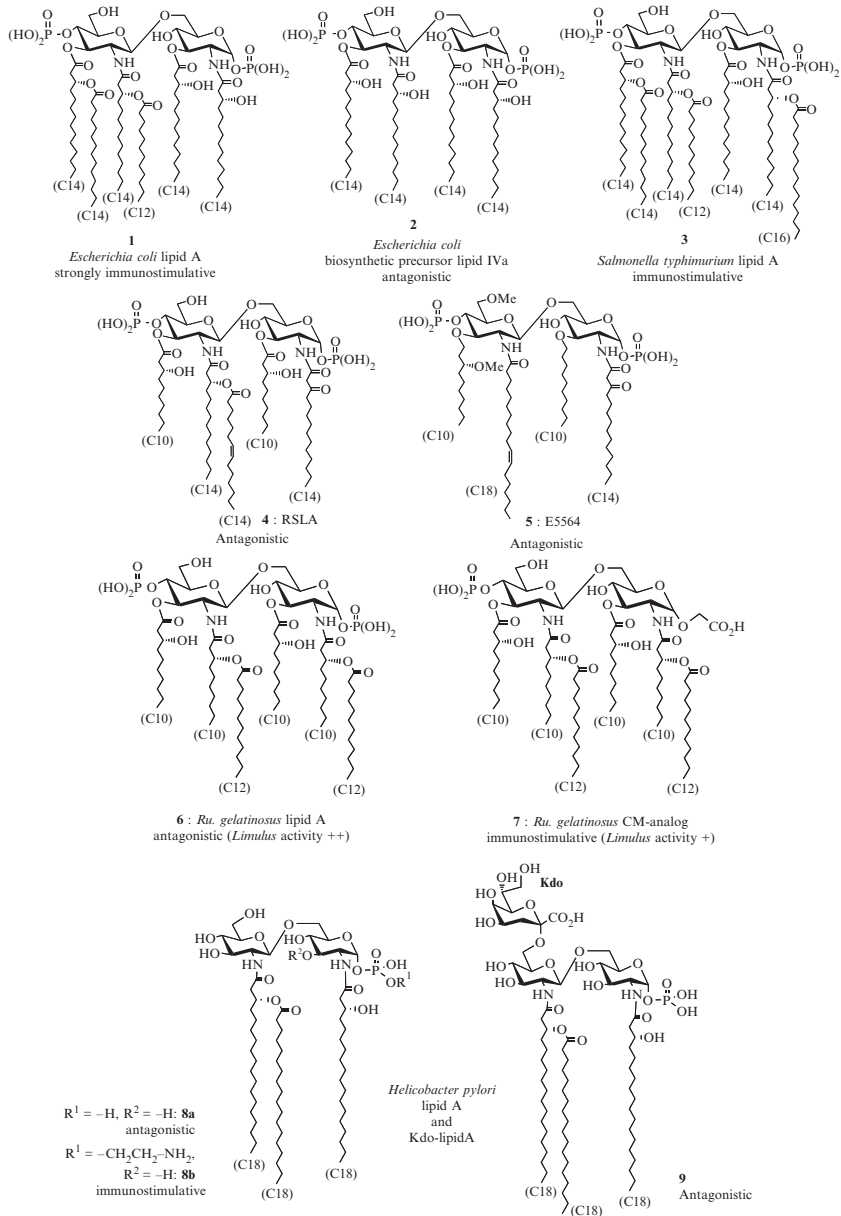


Figure 16.1 Structures of various lipid A and LPS partial structures.

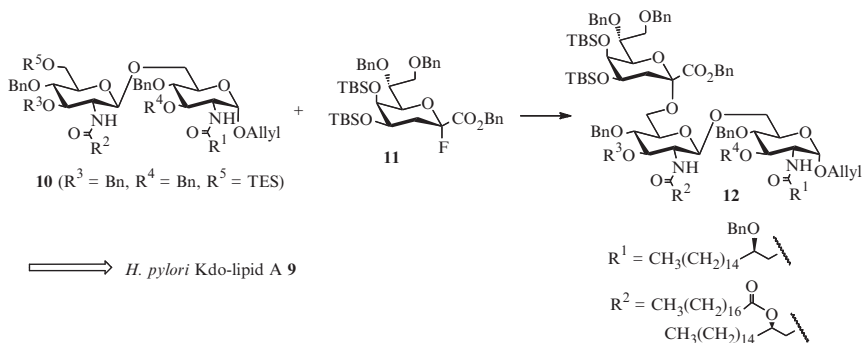


Figure 16.2 Synthesis of *Helicobacter pylori* Kdo–lipid A backbone.

3. SYNTHESIS OF *H. PYLORI* KDO–LIPID A BACKBONE

For the synthesis of Kdo–lipid A, the lipid A backbone (**10**) was first prepared, and connected with Kdo (**11**) with an α -selective glycosylation (Fig. 16.2) (Fujimoto *et al.*, 2007; Yoshizaki *et al.*, 2001). The molecular sieve 5A (MS5A) was found to be more effective for this reaction than MS4A, presumably because MS5A contains calcium, which traps fluoride anions and promotes glycosylation. The stereochemistry at the anomeric position was determined with the chemical shift of the protons at the 3'-position from ^1H NMR in comparison with the previously reported data (Fujimoto *et al.*, 2007; Yoshizaki *et al.*, 2001).

4. GLYCOSYLATION WITH KDO DONOR 11

- To a mixture of **10** (48.8 mg, 0.0275 mmol), Kdo-fluoride **11** (52.7 mg, 0.0713 mmol) and MS5A in dry CHCl_3 (2 mL) is added $\text{BF}_3 \cdot \text{OEt}_2$ (0.052 mL, 0.288 mmol) at -20°C and the mixture is stirred at -20°C for 1.5 h.
- After addition of saturated NaHCO_3 , the mixture is extracted with CHCl_3 . The organic layer is washed with saturated NaHCO_3 and brine, dried over anhydrous Na_2SO_4 , filtered, and concentrated under reduced pressure.
- The residue is purified by column chromatography (silica gel 50 g, $\text{CHCl}_3/\text{acetone} = 30/1$) to give **12** as a white solid (55.3 mg, 85%).

R_f ($\text{CHCl}_3/\text{acetone} = 30/1$) = 0.25; ESI-MS (positive) m/z 2402.51 $[[\text{M}+\text{Na}]^+]$; ^1H NMR (600 MHz, CDCl_3) δ = 7.35–7.20 (m, 40H, PhCH_2 8 \times), 6.24 (d, $J = 9.0$ Hz, 1H, NH), 5.96 (d, $J = 7.2$ Hz, 1H, NH'), 5.68 (m, 1H, $\text{OCH}_2\text{CH}=\text{CH}_2$), 5.17 (d, $J = 10.8$ Hz, 1H,

PhCH₂OCO), 5.15–5.13 (m, 1H, OCH₂CH=CH₂), 5.12–5.07 (m, 1H, OCH₂CH=CH₂), 5.04 (d, *J* = 10.8 Hz, 1H, PhCH₂OCO), 5.01 (d, *J* = 6.0 Hz, 1H, β-CH of acyloxyacyl), 4.97 (d, *J* = 7.8 Hz, 1H, H1'), 4.77 (d, *J* = 10.8 Hz, 1H, PhCH₂), 4.74–4.72 (m, 1H, PhCH₂), 4.70 (d, *J* = 3.7 Hz, 1H, H1), 4.69–4.67 (m, 1H, PhCH₂), 4.63 (d, *J* = 10.8 Hz, 1H, PhCH₂), 4.61 (d, *J* = 10.8 Hz, 1H, PhCH₂), 4.57 (d, *J* = 11.4 Hz, 1H, PhCH₂), 4.55 (d, *J* = 11.4 Hz, 2H, PhCH₂), 4.53 (d, *J* = 12.0 Hz, 1H, PhCH₂), 4.52 (d, *J* = 10.8 Hz, 1H, PhCH₂), 4.50 (d, *J* = 11.4 Hz, 1H, PhCH₂), 4.48 (d, *J* = 10.8 Hz, 1H, PhCH₂), 4.46 (d, *J* = 11.4 Hz, 1H, PhCH₂), 4.39 (d, *J* = 12.0 Hz, 1H, PhCH₂), 4.31–4.28 (m, 1H, H2), 4.24 (t, *J* = 8.5 Hz, 1H, H3'), 4.13–4.07 (m, 4H, H4'', H5'', H6'', OCH₂-CH=CH₂), 3.99–3.94 (m, 2H, H4, H7''), 3.89–3.87 (m, 2H, H6', H8''), 3.83 (d, *J* = 9.0 Hz, 1H, H5), 3.80–3.77 (m, 1H, β-CH of acyl), 3.73–3.63 (m, 6H, H3, H6 2×, H6', H8'', OCH₂-CH=CH₂), 3.59–3.56 (m, 1H, H5'), 3.39 (t, *J* = 8.5 Hz, 1H, H4'), 3.25 (q, *J* = 9.0 Hz, 1H, H2'), 2.34 (dd, *J* = 15.6, 7.2 Hz, 2H, α-CH₂ of acyloxyacyl, α-CH₂ of acyl), 2.25 (dd, *J* = 15.0, 7.8 Hz, 1H, α-CH₂ of acyl), 2.18 (dd, *J* = 15.6, 4.8 Hz, 1H, α-CH₂ of acyloxyacyl), 2.13–2.07 (m, 3H, OCOCH₂ of acyloxyacyl 2×, H3''), 1.96 (dd, *J* = 12.0, 3.6 Hz, 1H, H3''), 1.58–1.53 (m, 1H, γ-CH₂ of acyl), 1.48–1.45 (m, 2H, γ-CH₂ of acyl, OCOCH₂CH₂ of acyloxyacyl), 1.38 (q, *J* = 6.6 Hz, 1H, γ-CH₂ of acyloxyacyl), 1.31–1.04 (m, 82 H, CH₂ of acyl 82×), 0.92–0.82 (m, 27H, CH₃ of acyl 9×, *t*-BuSi 2×), 0.11–0.01 (m, 12H, CH₃Si 12×).

For obtaining the final compound, the anomeric position of trisaccharide was changed to the phosphate, and all the protecting groups were cleaved by hydrogenation (Fujimoto *et al.*, 2007).

5. CYTOKINE (IL-6) INDUCTION IN HUMAN PERIPHERAL WHOLE-BLOOD CELL CULTURES

1. The synthetic samples (lipid A **8a** and Kdo-lipid A **9** with noted concentrations in 25 μL of saline) and heparinized human peripheral whole-blood (HWBC) (25 μL) collected from an adult volunteer in RPM1 1640 medium (75 μL; Flow Laboratories, Irvine, Scotland, UK) are incubated in triplicate in a 96-well plastic plate at 37 °C in 5% CO₂. An LPS specimen prepared by Westphal method from *E. coli* O111:B4 (Sigma Chemicals Co.) is used as a positive control at the concentration of 0.5 ng/mL.
2. After 24 h of the incubation, the plate is centrifuged at 300×*g* for 2 min and cytokines in the supernatant are assayed (Suda *et al.*, 1995).
3. The levels of IL-6 induced by stimulating HWBC cultures with test samples are measured by means of an enzyme-linked immunosorbent assay (ELISA) using Human IL-6 ELISA kit (eBioscience, San Diego, CA, USA).

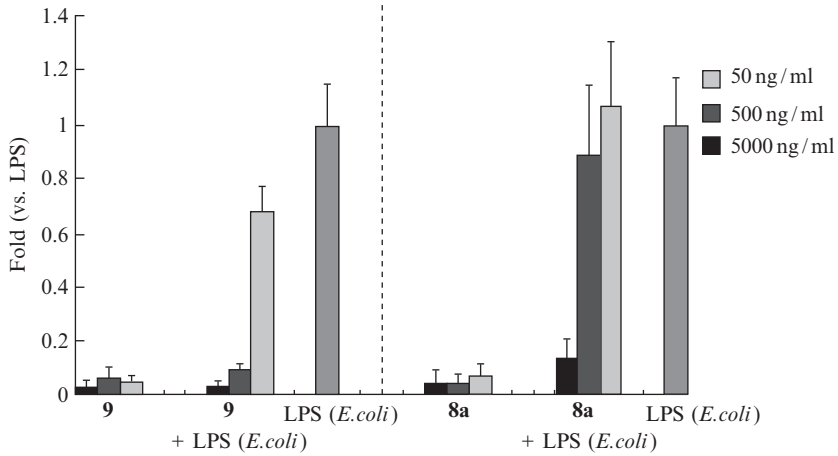


Figure 16.3 IL-6 induction and inhibition by *Helicobacter pylori* Kdo-lipid A **9** and lipid A **8a** with heparinized human peripheral whole-blood (HWBC). *E. coli* (O111:B4) LPS is used as a positive control at the concentration of 0.5 ng/mL.

Data represent averages of three repeated assays with standard deviations from individual experiments.

H. pylori Kdo-lipid A **9** and lipid A **8a** inhibited IL-6 induction by *E. coli* LPS. Kdo-lipid A **9** showed more potent antagonistic activity than **8a** (Fig. 16.3) (Fujimoto *et al.*, 2007). On the other hand, Lipid A **8b** having ethanolamine induced low levels of cytokines such as IL-18 and TNF- α via TLR4/MD-2 complex (Ogawa *et al.*, 2003). These results demonstrated that the number of anionic charges influences the biological activity of lipid A and LPS. Similar charge effects to biological activities were also observed in our studies of *Ru. gelatinosus* lipid A and lipid A analogs containing acidic amino acid residues (Fujimoto *et al.*, 2005). Immunostimulating or antagonistic activity can be controlled by the anionic charges in these analogs and *H. pylori* lipid A. The present study also explains why some strains of *H. pylori* LPS show weak immunostimulating activity, while others show antagonistic activity. Weak immunostimulating activity may be correlated with the ability of *H. pylori* to induce chronic inflammation, whereas the antagonistic activity should be important for suppressing the innate immune response and survival as a parasite.

6. BACTERIAL GLYCOCONJUGATES FOR NONSELF RECOGNITION—PEPTIDOGLYCAN (PGN)

PGN is a component of bacterial cell walls, and has conserved structural characteristics, which makes PGN fragment structures to be good motifs for nonself recognition. PGN has polysaccharide chains linked to

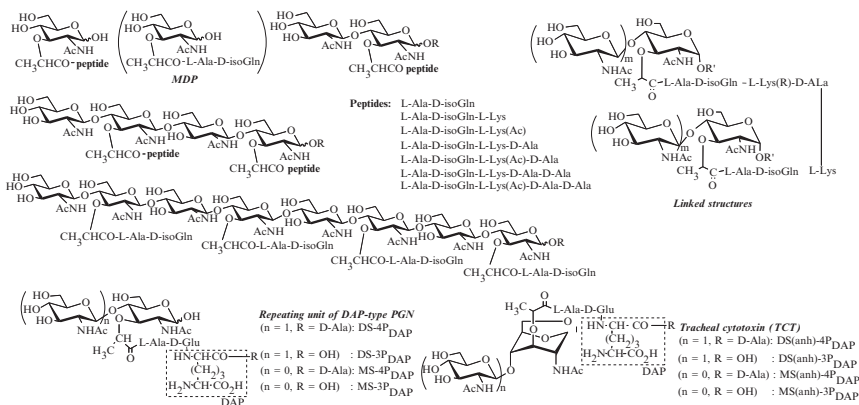


Figure 16.5 Chemically synthesized PGN fragment library (Inamura *et al.*, 2001, 2006; Kawasaki *et al.*, 2008; Kusumoto *et al.*, 2009).

that the MDP is a ligand of Nod2, which is another NLR family of intracellular proteins (Girardin *et al.*, 2003b; Inohara *et al.*, 2003).

We constructed the PGN fragments library (Fig. 16.5), which included Lys-type linear and linked fragments, and also DAP-type fragments such as a repeating unit of the PGN fragment (GlcNAc(β 1-4)MurNAc-L-Ala- γ -D-Glu-*meso*-DAP-D-Ala), tracheal cytotoxin (TCT; GlcNAc(β 1-4)MurNAc(anh)-L-Ala- γ -D-Glu-*meso*-DAP-D-Ala), and their fragments (Kawasaki *et al.*, 2008). The synthesis of TCT is shown in Fig. 16.6, and the one of the key reactions is the β -selective glycosylation as used to prepare **15** from glycosyl donor **13** and glycosyl acceptor **14**.

7. SYNTHESIS OF DISACCHARIDE MOIETY **15** IN TRACHEAL CYTOTOXIN WITH β -SELECTIVE GLYCOSYLATION

1. TMSOTf (5 ml, 0.030 mmol) is added to the solution of glucosamine imidate **13** (200 mg, 0.296 mmol), **14** (193.6 mg, 0.443 mmol), and MS4Å in dry CH_2Cl_2 (3 mL) at -17°C , and the mixture is stirred for 30 min under Ar atmosphere.
2. The reaction is quenched with saturated aqueous NaHCO_3 .
3. The organic layer is washed with brine, dried over Na_2SO_4 and concentrated *in vacuo*.
4. The residue is purified by silica-gel flash column chromatography (toluene/AcOEt = 7/1) to give **15** (182 mg, 65%).

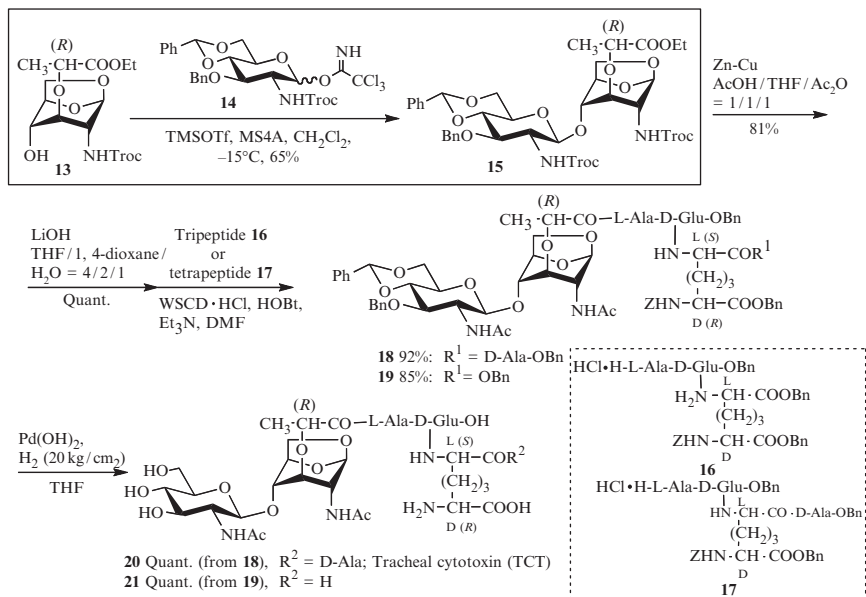


Figure 16.6 Synthesis of Tracheal cytotoxin (TCT) and its fragments. Abbreviations: Bn, benzyl; Tf, trifluoromethanesulfonyl; Troc, 2,2,2-trichloroethoxycarbonyl; TMS, trimethylsilyl; WSCD·HCl, 1-ethyl-3-(3-dimethylaminopropyl) carbodiimide hydrochloride; HOBT, 1-hydroxybenzotriazole; Z, benzyloxycarbonyl.

ESI-TOF-MS (positive) m/z 949.17 $[\text{M}+\text{H}]^+$; ^1H NMR (500 MHz, CDCl_3) δ = 7.52–7.18 (10H, m, ArH 2 \times), 5.60 (1H, s, Ph-CH=O_2), 5.33 (1H, s, $\text{H}_{\text{anh-1}}$), 5.03 (1H, d, J = 7.7 Hz, NH), 4.91 (1H, d, J = 12 Hz, $-\text{O-CH}_2\text{-Ph}$), 4.82 (1H, d, J = 8 Hz, H-1), 4.76 (2H, dd, J = 12 Hz, 20 Hz, $-\text{CH}_2\text{-CCl}_3$), 4.7 (1H, d, J = 12 Hz, $-\text{O-CH}_2\text{-Ph}$), 4.60 (1H, d, J = 12 Hz, NH), 4.49 (1H, d, J = 5.7 Hz, $\text{H}_{\text{anh-5}}$), 4.33 (1H, dd, J = 5 Hz, 10 Hz, H-6), 4.22 (1H, q, J = 3.6 Hz, Lac- α H), 4.20–4.14 (3H, m, $-\text{CH}_2\text{CH}_3$, $\text{H}_{\text{anh-6}'}$), 3.95 (1H, d, J = 9.8 Hz, $\text{H}_{\text{anh-2}}$), 3.86–3.76 (3H, m, H-3, H-6, H-4), 3.74–3.72 (2H, m, $\text{H}_{\text{anh-6}'}$, $\text{H}_{\text{anh-4}}$), 3.58 (1H, brs, $\text{H}_{\text{anh-3}}$), 3.52–3.42 (2H, m, H-2, H-5). Found: C, 47.02; H, 4.42; N, 2.96%. Calcd for $\text{C}_{37}\text{H}_{42}\text{Cl}_6\text{N}_2\text{O}_{14}$: C, 46.71; H, 4.45; N, 2.94%.

8. SYNTHESIS OF TRACHEAL CYTOTOXIN 20 AND ITS FRAGMENT 21

After preparation of the disaccharide **15**, 2,2,2-trichloroethoxycarbonyl (Troc) groups were changed to acetyl groups via cleavage of Troc group using Zn–Cu in the presence of acetic anhydride. The ethyl ester was cleaved

with LiOH, and then the liberated carboxyl group was connected to the DAP-containing peptides **16** or **17** by using 1-ethyl-3-(3-dimethylamino-propyl)carbodiimide (WSCD; water-soluble carbodiimide), 1-hydroxybenzotriazole (HOBt), and triethylamine (Et₃N) in DMF. After the coupling, all benzyl and benzyloxycarbonyl groups of **18** and **19** were removed by catalytic hydrogenation with Pd(OH)₂ and H₂ to give **20** (TCT) and **21** (Kawasaki *et al.*, 2008).

9. IMMUNOSTIMULATORY ACTIVITIES OF DAP CONTAINING PGN FRAGMENTS

The human Nod1 stimulating activity of the DAP-type synthetic PGN fragments have been evaluated by HEK293T bioassay expressed human Nod1 as previously described (Chamaillard *et al.*, 2003). In these compounds, **20** (TCT) shows only very weak human-Nod1 stimulatory activity, whereas **21** (DS(anh)-3P_{DAP}) shows approximately 10-fold higher activity than that of known ligand A-iE-DAP (Kawasaki *et al.*, 2008). These results are consistent with a report using TCT from a natural source (Magalhaes *et al.*, 2005), and demonstrate that a free carboxyl group at the 2-position of DAP is favorable for the human Nod1 recognition.

In case of human Nod1, TCT is a only weak stimulant, but it plays a fundamental role in innate immune systems of other species such as *Drosophila* with the activation of PGRP-LC (Kaneko *et al.*, 2004; Stenbak *et al.*, 2004). It has also been reported that recognition of DAP-type PGN by PGRP-LE in *Drosophila* is crucial for the induction of autophagy, which prevents intracellular growth of *Listeria monocytogenes* and promotes host survival after an infection (Yano *et al.*, 2008).

The structurally defined synthesized PGN fragments have been fundamental to understand the activation mechanism of innate immune system.

10. VISUALIZING THE *IN VIVO* DYNAMICS OF ANIMAL *N*-GLYCANS

Among the various types of oligosaccharide structures, asparagine-linked oligosaccharides (*N*-glycans) are the most prominent in terms of diversity and complexity. In particular, *N*-glycans containing sialic acid residues are involved in a variety of important physiological events, including cell-cell recognition, adhesion, signal transduction, and quality control (Kamerling *et al.*, 2007). Moreover, it has long been known that the sialic acids in *N*-glycans on soluble proteins or peptides enhance circulatory residence (Morell *et al.*, 1968), that is, *N*-glycan-engineered erythropoietin (EPO) (Elliott *et al.*, 2003) or insulin

(Sato *et al.*, 2004) exhibits a remarkably higher stability in serum, which effects the prolonged bioactivity. Antibody-dependent cellular cytotoxicity (ADCC) and/or complement-dependent cytotoxicity (CDC) has also been proposed to be modulated by the sialic acids of *N*-glycans in immunoglobulin (IgG) through Siglec interactions by glycosylating or removing the sialic acids (Kaneko *et al.*, 2006). However, these important findings and previous efforts in investigating *N*-glycan functions have been mostly based on *in vitro* experiments using isolated lectins, cultured cells, and dissected tissues. Recently, interest has shifted to the dynamics of these glycoproteins and/or glycans *in vivo*, that is, how the function and/or interaction of the individual *N*-glycan works synergistically through dynamic processes in the body to eventually exhibit biological phenomena. Molecular imaging (Tanaka and Fukase, 2008) is the most promising tool to visualize the “on-time” *N*-glycan dynamics *in vivo*. Although fluorescence imaging is the method of choice due to the convenient experimental and detection procedures at the small animal levels, magnetic resonance (MR), and more preferably, the positron emission tomography (PET) imaging, which have technologically improved sensitivity and resolution, are well suited for diagnostic applications. Nevertheless, molecular imaging of glycans has not been thoroughly examined, except for the ^{18}F -FDG tracer (technically a monosaccharide) and the very limited examples of liposome-conjugated oligosaccharides (Chen *et al.*, 2008; Hirai *et al.*, 2007). This is due to the lack of the efficient labeling methods of glycoproteins, and the bioactivity of the oligosaccharides is affected by the multivalency and/or heterogeneous environment, that is, on cell surfaces that are composed of oligosaccharide clusters along with other biomolecules. A single molecule of the *N*-glycan, either obtained from a natural or synthetic source, is readily excreted from the body (Vyas *et al.*, 2001). Thus, efficiently labeling and mimicking such a *N*-glycan-involved bioenvironment, for example, by conjugating the *N*-glycans, to the liposomes, or to the clusters, may provide information on the “*in vivo* dynamics” of *N*-glycans. Below we discuss the methods for microPET imaging of (1) glycoproteins and (2) dendrimer-type glycoclusters by making much use of the multivalency effects of 16 molecules of *N*-glycans.

11. PET IMAGING OF GLYCOPROTEINS

In order to investigate the effects of *N*-glycans, especially the sialic acid residue at the nonreducing end of the glycans, on the metabolic stability of the proteins, a microPET of glycoproteins, orosomucoid, and asialoorosomucoid could be investigated (Tanaka *et al.*, 2008). Based on the recently developed “azaelectrocyclization protocol” (Fig. 16.7A), glycoproteins available in only small amounts (62 μg of orosomucoid and

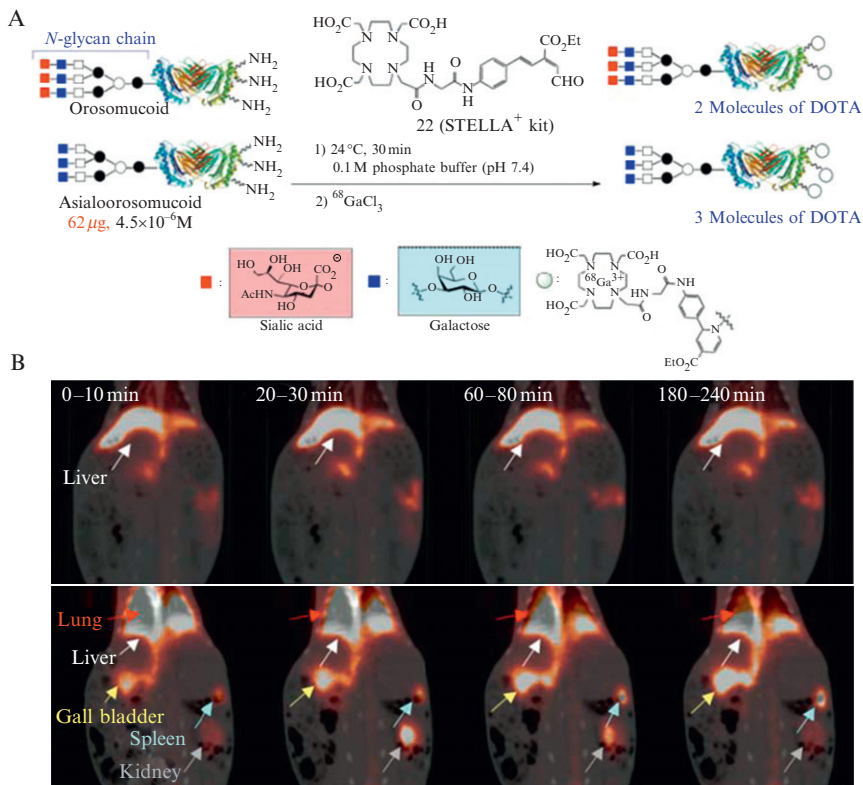


Figure 16.7 (A) Labeling of glycoproteins by DOTA by STELLA⁺ kit (B) Dynamic microPET images of [⁶⁸Ga]DOTA-glycoproteins in rabbits. Time course of accumulation of [⁶⁸Ga]DOTA-orosomuroid (upper) and [⁶⁸Ga]DOTA-asialorosomuroid (lower) in some peripheral organs (axial views). These PET images were fused to anatomical images obtained by using CT.

asialorosomuroid) were labeled with the incorporation of ~2–3 units of DOTA (1,4,7,10-tetraazacyclodecane-1,4,7,10-tetraacetic acid) by incubating the respective protein with aldehyde probe **22** (STELLA⁺, a kit available from Kishida, Co., Ltd.) for 30 min (Tanaka *et al.*, 2010). The DOTA-labeled glycoproteins were subsequently radiometallated with ⁶⁸Ga and their *in vivo* kinetics were analyzed in rabbit by means of microPET.

12. METHOD FOR ⁶⁸GA-DOTA LABELING AND MICROPET IMAGING IN RABBIT

1. PBS solutions of orosomuroid and asialorosomuroid (62 μg, 1.4 nmol, 295 μL, pH = 7.4) are reacted with a DMF solution of probe **22** (STELLA⁺ kit, 14 nmol, 1.5 μL) at room temperature for 30 min

- (reaction concentrations: 4.5×10^{-6} M for orosomuroid, 4.5×10^{-5} M for **22**).
2. DOTA-labeled proteins are purified by centrifugal filtration using Microcon[®] (Millipore, 30,000 cut).
 3. DOTA-proteins prepared above (10 μ g) are incubated with $^{68}\text{GaCl}_3$ solution (pH = 7.0, 1.68 mCi, 500 μ L) obtained from $^{68}\text{Ge}/^{68}\text{Ga}$ radionuclide generator, at 40 °C for 10 min.
 4. A solution of DOTA (1.0 μ mol, 10 mM in H₂O) is added in order to chelate and excrete the excess ^{68}Ga from the body during the PET study.
 5. ^{68}Ga -DOTA-glycoproteins at a dose of 15.8–16.1 MBq in 2.2 mL are injected via an ear vein of female Japanese white rabbits weighing 2.1–2.2 kg at 13 weeks of age (Japan SLC, Inc., Hamamatsu, Japan) under a general anesthesia with ketamine (60 mg/kg, Ketalar[®], Sankyo, Tokyo, Japan) and xylazine (6 mg/kg, Selactar[®], Bayer Yakuhin, Tokyo, Japan).
 6. During the imaging experiments, the rabbits are sedated continuously with intravenously administered a mixture of ketamine (60 mg/kg/h) and xylazine (6 mg/kg/hr).
 7. PET images are obtained by using a small animal PET scanner, the microPET P4 system (Siemens Medical Solutions Inc., Knoxville, TN, USA), and the emission data is collected for 240 min postinjection as 12 frames (6 \times 400 s, 3 \times 1000 s, 2 \times 1600 s, and 1 \times 3400 s), and is acquired with an energy window of 400–650 keV and a coincidence timing window of 6 ns.
 8. The images are reconstructed from 120 to 240 min after injection of ^{68}Ga -DOTA-orosomuroid or asialoorosomuroid by an ordered subset expectation maximization (OSEM) algorithm with attenuation correction using CT data or no scatter correction, and are smoothed by using a Gaussian kernel with an FWHM of 3 mm in the all directions.
 9. Quantitative analysis is performed using ASIPro VM version 6.3.3.0 software (Siemens Medical Solutions, Inc., Knoxville, TN, USA). Regions of interest (ROIs) are placed on the tissue region.

MicroPET images of ^{68}Ga -DOTA-orosomuroid and asialoorosomuroid in Fig. 16.7B detected the asialo-glycoprotein being cleared through-kidney faster than orosomuroid through the well-known asialoglycoprotein receptor (Morell *et al.*, 1968), thus achieving the visualization of sialic acid-dependent circulatory residence of glycoproteins. PET images also detected another clearance pathway of asialo-glycoprotein through the gallbladder, that is, intestinal excretion pathway, as well the accumulation to the lung and spleen. These promising PET images of glycoproteins suggest future uses for the glycoproteins in pharmacological and/or clinical applications.

13. PET IMAGING OF GLYCOCLUSTERS

In order to image the “*in vivo* dynamics” of glycans, it is necessary to mimic the “glycan-cluster environment,” as well as to make advantage of the glycan multivalency effects for the stronger interaction with lectins. The polylysine-based dendrimer-type glycoclusters **23a-c** with 16 molecules of glycans (Fig. 16.8) were developed as the excellent templates for investigating the *N*-glycan dynamics *in vivo* (Tanaka *et al.*, unpublished results); thus, the dendrimer core **23** with the *N*-benzyl histidine and the terminal acetylene embodied in the propargyl glycine residue (Fig. 16.8A) could be smoothly reacted with the 16 molecules of the azide-containing *N*-glycans with large and complex structures, that is, many hydroxyls and molecular weight of ca. 1500, based on the “self-activating” Huisgen 1,3-dipolar

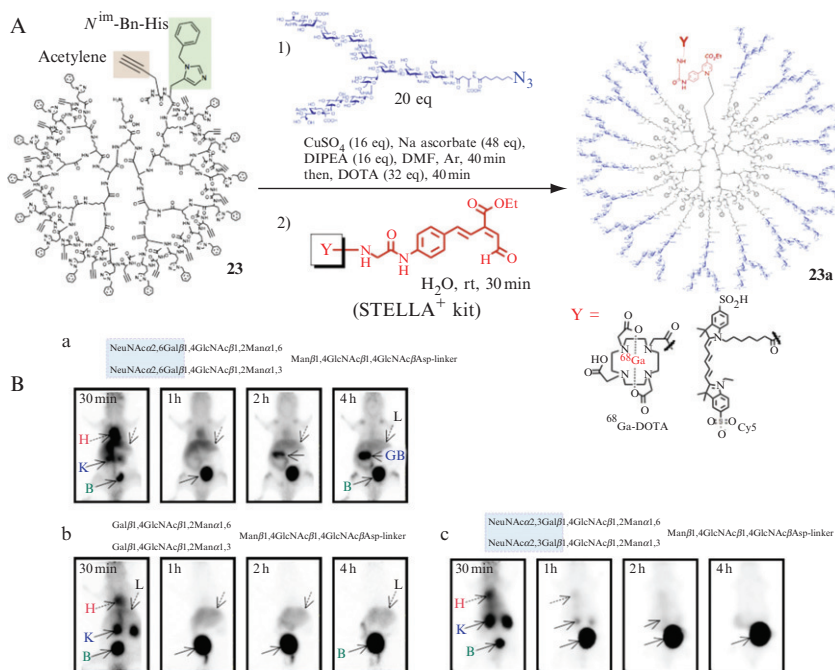


Figure 16.8 (A) Preparation of glycoclusters. (B) Dynamic PET imaging of glycoclusters **23a-c** in normal BALB/c nude mice. ⁶⁸Ga-DOTA-labeled glycoclusters (10 MBq) were administered from the tail vein of the mice ($n = 3$, 500 pmol, 100 μ L/mouse) and the whole body was scanned by a small animal PET scanner, microPET Focus 220 (Siemens Medical Solutions, Inc., Knoxville, TN, USA), over 0–4 h after injection; H, heart; K, kidney; L, liver; B, urinary bladder; GB, gallbladder. (a) glycocluster **23a**, (b) glycocluster **23b**, (c) glycocluster **23c**.

cycloaddition.” The clusters were designed to have a terminal lysine ε -amino group so that they could be efficiently labeled by ^{68}Ga -DOTA as the PET radiolabel, and if required, fluorescent groups, in the presence of numerous hydroxyls by labeling kit “STELLA⁺” under mild conditions (Tanaka *et al.*, unpublished results).

14. METHOD FOR PREPARATION OF *N*-GLYCAN CLUSTERS AND PET IMAGING IN MOUSE

1. Acetylene-containing polylysine **23** (16-mer, 158 μg , 2.0×10^{-5} mmol) is reacted with azide-containing *N*-glycans (1.0 mg, 4.0×10^{-4} mmol) in DMF (50 μL) and H_2O (50 μL) at room temperature in the presence of CuSO_4 (64 μg , 3.2×10^{-4} mmol), sodium L-ascorbate (238 μg , 1.2×10^{-3} mmol), and diisopropylethylamine (74 nL).
2. Excess copper ion is removed by chelating with DOTA (647 μg , 1.56×10^{-3} mmol) for 40 min at room temperature, and low-molecular weight compounds are filtered off using the centrifugal filtration by Microcon[®] (10,000 cut, Millipore).
3. Lyophilization of the aqueous solution and the purification by reverse-phase HPLC provide the desired glycoclusters.
4. Labeling by DOTA and ^{68}Ga , and MicroPET imaging were performed as described above, except using BALB/c mice for imaging (see Fig. 16.8 Caption).

Figure 16.8B shows the microPET in mice of the *N*-glycoclusters ($\text{Y} = ^{68}\text{Ga}$ -DOTA) with the glycan structure of bis-Neu α (2-6)Gal glycan **23a**, asialo-glycan **23b**, and bis-Neu α (2-3)Gal glycan **23c**. ^{68}Ga -radioactivity derived from **23a** was retained after 4 h in the liver (Fig. 16.8B (a)), and was excreted slowly from the kidney/urinary bladder and from the gallbladder (intestinal excretion pathway). On the other hand, asialo-glycan cluster **23b** rapidly cleared through the kidney to the bladder (Fig. 16.8B(b)), although some accumulation was observed in the liver because the asialoglycoprotein receptors are highly expressed in this organ (Morell *et al.*, 1968). The results are consistent with the PET analyses of glycoproteins discussed above (Tanaka *et al.*, 2008), where the asialo-congener is more rapidly excreted than orosomucoid through the kidney. However, the α -linking to the 3-OH of galactose in glycocluster **23c**, which also contains sialic acid, was readily excreted through the kidney/urinary bladder as shown in Fig. 16.8B(c). These PET results on the 16-mer glycoclusters **23a-c** suggest that the specific sialoside linkage to galactose, that is, Neu α (2-6)Gal linkage, in *N*-glycan structures plays an important role in the circulatory residence of *N*-glycans, which in turn

results in uptake of **23a** in the liver. In addition, this specific sialoside linkage markedly differentiates the excretion mechanism from those of the asialo- and Neu α (2-3)Gal cases, which proceed via a biofiltration pathway through the kidney.

The notable difference in the serum stability due to the sialoside bond linkages to the galactose, that is, the α (2-6)- versus α (2-3)-linkages, is an intriguing observation. These dynamic PET images suggest a new receptor-mediated excretion mechanism for Neu α (2-3)Gal-containing glycans. Namely, Neu α (2-3)Gal-cluster **23c**, which usually cannot be found in serum, is probably recognized as an invader and smoothly excreted by the vascular endothelial cells, erythrocytes, leucocytes, and via the phagocytosis by a macrophage; the smaller sized degradation products may be filtered in the kidney. Alternatively, the “excretion-escaping” mechanism by stimulating the immunosuppressive signals through the ITIM (immunoreceptor tyrosine-based inhibitory motif) molecules via Siglec families (Varki and Angata, 2006), may account for the higher stability of Neu α (2-6)Gal-glycan. It is reported that the Neu α (2-6)Gal-containing BSA reduces but does not prevent binding to the asialoglycoprotein receptor, while the Neu α (2-3)Gal-congener abolishes the binding (Park *et al.*, 2005). Therefore, the prolonged half-life coupled to uptake by the asialoglycoprotein receptor account for the high accumulation of **23a** in the liver (Fig. 16.8B(a)). Biantennary Neu α (2-6)Gal-chains especially reduce binding in comparison with tri- and tetraantennary glycans (Lee *et al.*, 1983), nevertheless, the combination of high valency and long circulatory half life (reduced clearance) likely leads to the uptake of **23a** by hepatocytes via the Gal/GalNAc lectin receptor. Note that the slow clearance of bis-Neu α (2-6)Gal cluster **23a** through the gallbladder may be due to the “polar transport mechanism” (Nakagawa *et al.*, 2006), which “tags” the fucose to specific *N*-glycans in the liver. Elucidation of a detailed mechanism will be the subject of future investigations.

ACKNOWLEDGMENTS

This work was supported in part by Grants-in Aid for Scientific research (No. 19310144, 19681024, 19651095, and 20241053) from Japan Society for the Promotion of Science, by grants from the Institute for Fermentation, Osaka (IFO), Collaborative Development of Innovative Seeds from Japan Science and Technology Agency (JST), New Energy and Industrial Technology Development Organization (NEDO, project ID: 07A01014a), Research Grants from Yamada Science Foundation as well as Molecular Imaging Research Program, Grants-in-Aid for Scientific Research from the Ministry of Education, Culture, Sports, Science and Technology (MEXT) of Japan.

REFERENCES

- Chamaillard, M., Hashimoto, M., Horie, Y., Masumoto, J., Qiu, S., Saab, L., Ogura, Y., Kawasaki, A., Fukase, K., Kusumoto, S., Valvano, M. A., Foster, S. J., *et al.* (2003). An essential role for NOD1 in host recognition of bacterial peptidoglycan containing diaminopimelic acid. *Nat. Immunol.* **4**, 702–707.
- Chen, W. C., Completo, G. C., and Paulson, J. C. (2008). Targeting of human B lymphoma with cytotoxic liposomes containing glycan ligands of CD22. *Glycobiology* **18**, 963.
- Elliott, S., Lorenzini, T., Asher, S., Aoki, K., Brankow, D., Buck, L., Busse, L., Chang, D., Fuller, J., Grant, J., Hernday, N., Hokum, M., *et al.* (2003). Enhancement of therapeutic protein in vivo activities through glycoengineering. *Nat. Biotechnol.* **21**, 414–421.
- Fujimoto, Y., Adachi, Y., Akamatsu, M., Fukase, Y., Kataoka, M., Suda, Y., Fukase, K., and Kusumoto, S. (2005). Synthesis of lipid A and its analogues for investigation of the structural basis for their bioactivity. *J. Endotoxin Res.* **11**, 341–347.
- Fujimoto, Y., Iwata, M., Imakita, N., Shimoyama, A., Suda, Y., Kusumoto, S., and Fukase, K. (2007). Synthesis of immunoregulatory *Helicobacter pylori* lipopolysaccharide partial structures. *Tetrahedron Lett.* **48**, 6577–6581.
- Girardin, S. E., Boneca, I. G., Carneiro, L. A., Antignac, A., Jehanno, M., Viala, J., Tedin, K., Taha, M. K., Labigne, A., Zähringer, U., Coyle, A. J., DiStefano, P. S., *et al.* (2003a). Nod1 detects a unique muropeptide from gram-negative bacterial peptidoglycan. *Science* **300**, 1584–1587.
- Girardin, S. E., Boneca, I. G., Viala, J., Chamaillard, M., Labigne, A., Thomas, G., Philpott, D. J., and Sansonetti, P. J. (2003b). Nod2 is a general sensor of peptidoglycan through muramyl dipeptide (MDP) detection. *J. Biol. Chem.* **278**, 8869–8872.
- Hirai, M., Minematsu, H., Kondo, N., Oie, K., Igarashi, K., and Yamazaki, N. (2007). Accumulation of liposome with Sialyl Lewis X to inflammation and tumor region: Application to in vivo bio-imaging. *Biochem. Biophys. Res. Commun.* **353**, 553–558.
- Inamura, S., Fukase, K., and Kusumoto, S. (2001). Synthetic study of peptidoglycan partial structures. Synthesis of tetrasaccharide and octasaccharide fragments. *Tetrahedron Lett.* **42**, 7613–7616.
- Inamura, S., Fujimoto, Y., Kawasaki, A., Shiokawa, Z., Woelk, E., Heine, H., Lindner, B., Inohara, N., Kusumoto, S., and Fukase, K. (2006). Synthesis of peptidoglycan fragments and evaluation of their biological activity. *Org. Biomol. Chem.* **4**, 232–242.
- Inohara, N., Ogura, Y., Fontalba, A., Gutierrez, O., Pons, F., Crespo, J., Fukase, K., Inamura, S., Kusumoto, S., Hashimoto, M., Foster, S. J., Moran, A. P., *et al.* (2003). Host recognition of bacterial muramyl dipeptide mediated through NOD2. Implications for Crohn's disease. *J. Biol. Chem.* **278**, 5509–5512.
- Kamerling, J. P., Boons, G. J., Lee, Y. C., Suzuki, A., Taniguchi, N., and Voragen, A. G. J. (2007). Analysis of glycans, polysaccharide functional properties & biochemistry of glycoconjugate glycans, carbohydrate-mediated interactions. *Comprehensive Glycoscience, From Chemistry to Systems Biology, Vol II & III*, Elsevier, UK.
- Kaneko, T., Goldman, W. E., Mellroth, P., Steiner, H., Fukase, K., Kusumoto, S., Harley, W., Fox, A., Golenbock, D., and Silverman, N. (2004). Monomeric and polymeric gram-negative peptidoglycan but not purified LPS stimulate the *Drosophila* IMD pathway. *Immunity* **20**, 637–649.
- Kaneko, Y., Nimmerjahn, F., and Ravetch, J. V. (2006). Anti-inflammatory activity of immunoglobulin G resulting from Fc sialylation. *Science* **313**, 670–673.
- Kawasaki, A., Karasudani, Y., Otsuka, Y., Hasegawa, M., Inohara, N., Fujimoto, Y., and Fukase, K. (2008). Synthesis of diaminopimelic acid-containing peptidoglycan fragments and tracheal cytotoxin (TCT) for investigation of their biological functions. *Chem. Eur. J.* **14**, 10318–10330.

- Kusumoto, S., and Fukase, K. (2006). Synthesis of endotoxic principle of bacterial lipopolysaccharide and its recognition by the innate immune systems of hosts. *Chem. Rec.* **6**, 333–343.
- Kusumoto, S., Fukase, K., and Oikawa, M. (1999). The chemical synthesis of lipid A. *Endotoxin Health Dis.* 243–256.
- Kusumoto, S., Fukase, K., and Fujimoto, Y. (2009). Chemical synthesis of bacterial lipid A. *Microb. Glycobiol.: Struct. Relevance Appl.* 415–427.
- Lee, Y. C., Townsend, R. R., Hardy, M. R., Lonngren, J., Arnarp, J., Haraldsson, M., and Lonn, H. (1983). Binding of synthetic oligosaccharides to the hepatic Gal/GalNAc lectin. Dependence on fine structural features. *J. Biol. Chem.* **258**, 199–202.
- Magalhaes, J. G., Philpott, D. J., Nahori, M. A., Jehanno, M., Fritz, J., Le Bourhis, L., Viala, J., Hugot, J. P., Giovannini, M., Bertin, J., Lepoivre, M., Mengin-Lecreulx, D., et al. (2005). Murine Nod1 but not its human orthologue mediates innate immune detection of tracheal cytotoxin. *EMBO Rep.* **6**, 1201–1207.
- Morell, A. G., Irvine, R. A., Sternlieb, I., Scheinberg, I. H., and Ashwell, G. (1968). Physical and chemical studies on ceruloplasmin V. Metabolic studies on sialic acid-free ceruloplasmin in vivo. *J. Biol. Chem.* **243**, 155–159.
- Nakagawa, T., Uozumi, N., Nakano, M., Mizuno-Horikawa, Y., Okuyama, N., Taguchi, T., Gu, J., Kondo, A., Taniguchi, N., and Miyoshi, E. (2006). Fucosylation of N-glycans regulates the secretion of hepatic glycoproteins into bile ducts. *J. Biol. Chem.* **281**, 29797–29806.
- Ogawa, T., Asai, Y., Sakai, Y., Oikawa, M., Fukase, K., Suda, Y., Kusumoto, S., and Tamura, T. (2003). Endotoxic and immunobiological activities of a chemically synthesized lipid A of *Helicobacter pylori* strain 206-1. *FEMS Immunol. Med. Microbiol.* **36**, 1–7.
- Park, E. I., Mi, Y., Unverzagt, C., Gabius, H. J., and Baenziger, J. U. (2005). The asialoglycoprotein receptor clears glycoconjugates terminating with sialic acid alpha 2, 6GalNAc. *Proc. Natl. Acad. Sci. USA* **102**, 17125–17129.
- Raetz, C. R., and Whitfield, C. (2002). Lipopolysaccharide endotoxins. *Annu. Rev. Biochem.* **71**, 635–700.
- Sakai, Y., Oikawa, M., Yoshizaki, H., Ogawa, T., Suda, Y., Fukase, K., and Kusumoto, S. (2000). Synthesis of *Helicobacter pylori* lipid A and its analogue using p-(trifluoromethyl) benzyl protecting group. *Tetrahedron Lett.* **41**, 6843–6847.
- Sato, M., Furuike, T., Sadamoto, R., Fujitani, N., Nakahara, T., Niikura, K., Monde, K., Kondo, H., and Nishimura, S. (2004). Glycoinsulins: Dendritic sialyloligosaccharide-displaying insulins showing a prolonged blood-sugar-lowering activity. *J. Am. Chem. Soc.* **126**, 14013–14022.
- Schleifer, K. H., and Kandler, O. (1972). Peptidoglycan types of bacterial cell walls and their taxonomic implications. *Bacteriol. Rev.* **36**, 407–477.
- Stenbak, C. R., Ryu, J. H., Leulier, F., Pili-Floury, S., Parquet, C., Herve, M., Chaput, C., Boneca, I. G., Lee, W. J., Lemaitre, B., and Mengin-Lecreulx, D. (2004). Peptidoglycan molecular requirements allowing detection by the *Drosophila* immune deficiency pathway. *J. Immunol.* **173**, 7339–7348.
- Suda, Y., Tochio, H., Kawano, K., Takada, H., Yoshida, T., Kotani, S., and Kusumoto, S. (1995). Cytokine-inducing glycolipids in the lipoteichoic acid fraction from *Enterococcus hirae* ATCC 9790. *FEMS Immunol. Med. Microbiol.* **12**, 97–112.
- Takada, H., and Kotani, S. (1992). Vol: I Molecular Biochemistry and Cellular Biology. CRC Press, Boca Raton.
- Tanaka, K., and Fukase, K. (2008). PET (positron emission tomography) imaging of biomolecules using metal-DOTA complexes: A new collaborative challenge by chemists, biologists, and physicians for future diagnostics and exploration of in vivo dynamics. *Org. Biomol. Chem.* **6**, 815–828.

- Tanaka, K., Masuyama, T., Hasegawa, K., Tahara, T., Mizuma, H., Wada, Y., Watanabe, Y., and Fukase, K. (2008). A submicrogram-scale protocol for biomolecule-based PET imaging by rapid 6 Π -azaelectrocyclization: visualization of sialic acid dependent circulatory residence of glycoproteins. *Angew. Chem. Int. Ed.* **47**, 102–105.
- Tanaka, K., Minami, K., Tahara, T., Fujii, Y., Siwu, E. R. O., Nozaki, S., Onoe, H., Yokoi, S., Koyama, K., Watanabe, Y., Fukase, K. (2010). Electrocyclization-based labeling allows efficient *in vivo* imaging of cellular trafficking. *ChemMedChem.* **5**, 841–845.
- Varki, A., and Angata, T. (2006). Siglecs—The major subfamily of I-type lectins. *Glycobiology* **16**, 1R–27R.
- Vyas, S. P., Singh, A., and Sihorkar, V. (2001). Ligand-receptor-mediated drug delivery: An emerging paradigm in cellular drug targeting. *Crit. Rev. Ther. Drug Carrier Syst.* **18**, 1–76.
- Yano, T., Mita, S., Ohmori, H., Oshima, Y., Fujimoto, Y., Ueda, R., Takada, H., Goldman, W. E., Fukase, K., Silverman, N., Yoshimori, T., and Kurata, S. (2008). Autophagic control of listeria through intracellular innate immune recognition in *Drosophila*. *Nat. Immunol.* **9**, 908–916.
- Yoshizaki, H., Fukuda, N., Sato, K., Oikawa, M., Fukase, K., Suda, Y., and Kusumoto, S. (2001). First total synthesis of the Re-type lipopolysaccharide. *Angew. Chem. Int. Ed. Engl.* **40**, 1475–1480.